Facile and High-Throughput Synthesis of Functional Microparticles with Quick Response Codes

*Lisa Marie S. Ramirez, Muhan He, Shay Mailloux, Justin George, and Jun Wang**

***E**ncoded microparticles are high demand in multiplexed assays and labeling. However, the current methods for the synthesis and coding of microparticles either lack robustness and reliability, or possess limited coding capacity. Here, a massive coding of dissociated elements (MiCODE) technology based on innovation of a chemically reactive off-stoichimetry thiol-allyl photocurable polymer and standard lithography to produce a large number of quick response (QR) code microparticles is introduced. The coding process is performed by photobleaching the QR code patterns on microparticles when fluorophores are incorporated into the prepolymer formulation. The fabricated encoded microparticles can be released from a substrate without changing their features. Excess thiol functionality on the microparticle surface allows for grafting of amine groups and further DNA probes. A multiplexed assay is demonstrated using the DNA-grafted QR code microparticles. The MiCODE technology is further characterized by showing the incorporation of BODIPY-maleimide (BDP-M) and Nile Red fluorophores for coding and the use of microcontact printing for immobilizing DNA probes on microparticle surfaces. This versatile technology leverages mature lithography facilities for fabrication and thus is amenable to scale-up in the future, with potential applications in bioassays and in labeling consumer products.*

1. Introduction

2D quick response (QR) codes are commonly seen on commercial commodities as microtaggants for anticounterfeiting, labels for inventory control and pricing information, and storage for data collection. In molecular biology, generating miniaturized codes with a great variety of shapes and formats has also been the prevailing technique for labeling and performing multiplexed assays. These codes are normally carried by microparticles and macromolecules as a suspension array and are used in gene expression studies, drug screening, and clinical diagnostics to distinguish between various molecular binding events.[1–6] Different from conventional arrays on a glass slide where the array elements could be separated by their spatial addresses, the elements for a suspension array in an aqueous solution need unique embedded codes to be identified. For sensing purposes, the use of encoded microparticles is advantageous in that they offer higher flexibility in detection strategies and faster reaction kinetics in solution compared to those fixed on a solid substrate.[7–11]

Despite the usefulness of encoded microparticles in multiplexed bioassays and the multitude of available platforms for their synthesis, there are only a few examples of success in the commercialization of encoded microparticles.[12]

L. M. S. Ramirez, M. He, Dr. S. Mailloux, J. George, Prof. J. Wang
Multiplex Biotechnology Laboratory
Department of Chemistry
University at Albany
State University of New York
Albany, NY 12222, USA
E-mail: jwang34@albany.edu
Prof. J. Wang
Cancer Research Center
University at Albany
State University of New York
Rensselaer, NY 12144, USA

DOI: 10.1002/smll.201600456

Manufacturing of such microparticles still largely remains at the development stage, possibly because of the complexity involved in scaling up processes for particle synthesis and coding. The Luminex assay, which serves as a representative commercialized technology based on encoded microbeads, can achieve a multiplexity up to ≈500 analytes per sample. However, Luminex microbeads are monofunctional and contain no further information aside from fluorophore and color intensity combinations. Furthermore, Luminex assay expenses may impede its use in high-throughput screening applications. Several microfluidics-based methods have been utilized to produce encoded microparticles in a laboratory setting. Stop-flow lithography (SFL) has been used to synthesize particles bearing codes such as unpolymerized holes of different geometries, and also color-coded regions defined by the incorporation of fluorophores into the particle's polymer matrix.[13–17] Another popular platform is droplet microfluidics, which has been used to produce encoded microspheres with different combinations of dyes.[18] Optofluidic lithography has also allowed for the production of shape-encoded particles, as well as rendering of complex gradational micropatterns on particles that have been used to render intricate images on particles.[19–22] This method has been used to incorporate high-capacity QR codes on polymer microtaggants.[22] However, the scale-up of these microfluidics-based strategies might be complicated by setting up automated microfluidic systems with precise placement of UV projection systems for creating codes. The combination of programmable projection and microfluidic chip can potentially address the automation issue to create individualized microparticles in a high-throughput fashion.[23] Alternatively, some approaches based on conventional photolithography and new biomaterials without autofluorescence for encoding and bioassays have been introduced, although the multiplexity is limited.[24,25] Other encoding mechanisms such as graphical and electronic encoding are limited either by the complexity and throughput of production, the speed and robustness of the readout procedure, or by the functionality of the particles for downstream applications.[12,26]

A unified, versatile technology that possesses multiple advantages of the aforementioned microtechnologies and surpasses their limitations has a high demand in bioassay development and consumer product labeling. First, the ideal encoded particles should be fabricated in a high-throughput fashion utilizing the current facility infrastructure, so that the production is amenable to scale-up in the future. Photolithography based on photoresists is one of the most widely used industrial techniques for micropattern fabrication, thus, a photolithographic approach to synthesis of encoded particles would be highly compatible with existing well-established facilities in the semiconductor industry. Moreover, photolithography brings added precision to rendering of microstructures, thus a multitude of geometries and coding capabilities may be explored.[24,27] Second, the ideal encoded particles should be generated with high-capacity coding and unique code(s) for each element, and the readout should be quick and convenient. The optimization of the decoding process for encoded microparticles may introduce a bottleneck in developing commercialized assays, thus it is highly useful to develop encoded particles that can easily be read or decoded by existing software. 2D QR codes can store a large amount of identification information including numerical and alphanumeric data in multiple languages, and can be read by cellphones or many computer programs. However, the fabrication of QR barcode microparticles is technically challenging so only a few related works have been reported.[22] Finally, for bioassay purposes, the ideal encoded particles should be easy to functionalize so that oligonucleotides or antibodies may be grafted on the particles. Photoresist materials are mostly not chemically reactive and therefore are not suitable for biomolecule immobilization.

To address the demand for producing particles not only with a scalable fabrication process but also with high coding capacity for multiplexed bioassay applications, we developed and characterized a novel photolithography-based microtechnology for producing encoded microparticles. This technology, termed massive coding of dissociated elements, or MiCODE, leverages the conventional photolithography facilities to provide a virtually unlimited number of unique codes, and is suitable for future industrial-level manufacturing. MiCODE particles may be fabricated utilizing the current photolithography facility infrastructures in the semiconductor industry, so that the production is amenable to scale-up. With the MiCODE technology, it is possible to designate n codes to n particles using just a single patterning step, and the number of codes is only limited by the design of the code-patterned photomask and the size of the lithography substrate.

We exploited thiol-ene chemistry for generating MiCODE particles because this chemistry affords multiple key advantages over other existing photocurable materials. Compared to photoresists such SU-8 and 1002F, our thiol-ene photopolymer has lower (≈0) autofluorescence, thus it may find uses in fluorescence-based bioassays. In contrast to hydrogel photopolymers such as poly(ethylene) glycol diacrylate (PEG-DA), the thiol-ene polymer maintains its structural and mechanical integrity with or without immersion in aqueous media, thus the codes on MiCODE particles can be read without needing to swell the particles in water. The thiol-ene system also has low sensitivity to oxygen inhibition, thus allowing for handling under usual laboratory conditions without inert atmospheres.[28] Intact chemical reactivity of thiol-ene particles after lithography also allows for potential bioconjugation reactions with excess thiol groups on the particle surface. Thiol-based reactions have found wide utility in bioconjugations, thus thiol-functionalized microparticles may be useful in biological and clinical applications.[29]

In this report, we show the photolithographic fabrication of thiol-ene MiCODE microparticles that can be released into aqueous media such as commonly used buffers with full structural integrity as well as thiol groups available on the surface for grafting with biomolecules. We demonstrate a facile encoding strategy based on photobleaching of MiCODE particles incorporated with Nile Red or BDP-M dyes. With this photobleaching approach, high-capacity QR codes are patterned onto MiCODE particles in a single UV exposure step, in order to overcome the limitation of multiplexity and increase the volume of information. This encoding method has a throughput of thousands to millions per batch,

DOI: 10.1002/smll.201600456

and produces 21-bit to 49-bit QR codes that are readable by cellphone apps. We demonstrate the functionalization of the encoded microparticles with DNA probes, and the subsequent use of these microparticles in the multiplexed detection of oligo complementary DNAs. We envision that MiCODE particles can find broad applications in high-throughput drug screening, medical diagnostics, analysis of genetic and signaling information, as well as in labeling consumer goods for information storage or anti-counterfeiting measures.

2. Results and Discussion

In this work, we demonstrate a facile synthesis of encoded microparticles based on a photolithography with a thiol-ene system acting as a negative "photoresist." The microparticle fabrication from this material is based on a step-growth polymerization procedure[30,31] using a tetra-thiol monomer (PETMP) and a tri-allyl monomer (TATATO) with a 2-hydroxy-2-methylpropiophenone photoinitiator (HMPP) (**Figure 1**a). After surveying an array of chemicals and photoinitiators as alternatives to commercial photoresists, we decided to use a thiol-ene formulation as an appropriate photopolymerizable structural material for lithography because this system possesses a few advantages over other photocurable polymers. The thiol-ene polymer can form small features on the order of 100 nm.[32] In general, thiol-ene systems have high curing rates,[28] and in this work our thiol-ene formulation was able to polymerize in less than 20 s (fabrication details are found in the Experimental Section). The thiol-ene polymerization process also has low sensitivity to oxygen inhibition and is robust.[28] Thus our photolithography-based synthesis was carried out under ambient oxygen levels. Moreover, previous work has shown that the thiol-ene polymer has low shrinkage stress[33,34] as well as good mechanical strength,[35] which made the system attractive for applications in encoded microparticle synthesis.

In general, thiol-ene photopolymers feature tunable mechanical properties depending on the structure and ratio of thiol and ene monomers.[35] By choosing a formulation with an excess thiol to allyl ratio at 1.6:1, we were able to maintain sufficient thiol groups on the surface of the particles for further modification or functionalization. Excess thiol formulation also resulted in better shape in the overall fabrication procedure for features >100 μm (Table S2, Supporting Information). Our formulation shows similar fabrication capabilities comparable to commercial photoresists, as microparticles ranging in size from 15 to 330 μm with a thickness of ≈15–20 μm (Figure 1b,c) were uniformly patterned on glass slides or silicon wafers. Square and cubic particles were specifically chosen to demonstrate the effective fabrication of sharp features and distinct edges, which would not be obvious if round or cylindrical features were used. We have also shown multilayer fabrication of 3D structures (Figure S1, Supporting Information), which may

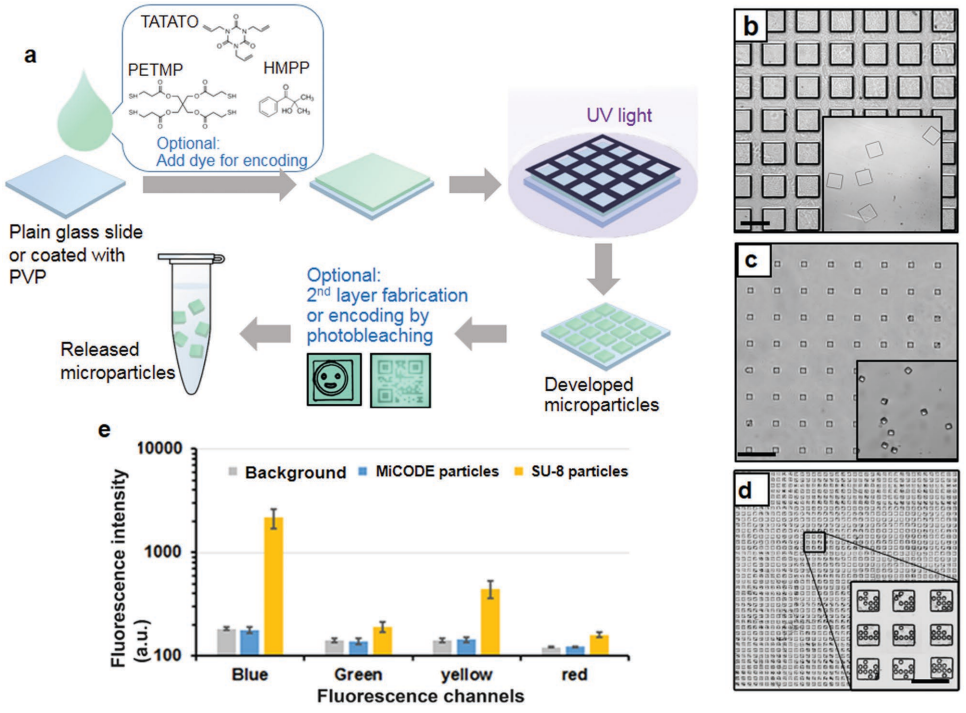

Figure 1. a) General scheme for fabrication of MiCODE elements. The custom prepolymer comprised of PETMP, TATATO, and HMPP (with optional addition of fluorescent dye) is patterned on a glass surface or a sacrificial layer following standard lithography to form a microparticle array. Additional layers may be fabricated using the same strategy, and fluorophore-containing particles may be subjected to encoding by photobleaching. Particles fabricated on plain glass slides are lifted off and suspended in a solution. Square microparticles with the sizes of b) 330 μm and c) 15 μm were patterned on a glass slide. The inset pictures are the respective lifted microparticles resuspended in PBS. Scale bars are b) 500 μm and c) 100 μm. d) Encoding 290 μm MiCODE microparticles by 16-bit binary arrays. Scale bar is 500 μm. e) Autofluorescence of MiCODE particles and SU-8 particles at various fluorescence wavelengths. Background fluorescence was taken from a plain glass slide without particles. Error bars denote standard deviation (n = 3).

DOI: 10.1002/smll.201600456

be used to give the microparticles unique identities and enrich the encoding approaches, as complex structures of microparticles are also useful for incorporating codes.[6,36]

The fabrication processes for microparticles using this new thiol-ene "photoresist" were optimized by fine-tuning spin-coating parameters, UV illumination intensity and exposure time, and post-exposure procedures (Table S1, Supporting Information). The general procedures are outlined in Figure 1a. In a representative fabrication, the thiol-ene prepolymer mixture is first prepared from PETMP, TATATO, and HMPP; this base mixture may be incorporated with fluorescent dye for downstream encoding processes based on photobleaching. The prepolymer is spun on a glass or silicon substrate and exposed to collimated UV light through a photomask. The pattern is then developed, where the unexposed monomers are dissolved and removed from the solid substrate, leaving behind a distinct array pattern of cross-linked thiol-ene polymer with well-defined shapes (Figure S2, Supporting Information). The arrays bearing different codes can be segmented into small regions for individual chemical treatment. The so-called "microparticle arrays" can be encoded in situ (i.e., as the microparticles are being synthesized) or after microparticle synthesis by photobleaching fluorophores incorporated into the microparticle polymer matrix. The various ways of encoding are discussed in the following sections. After synthesis and encoding, microparticles are then released into different media. Using this photolithography-based approach, we have fabricated microparticles of various sizes and features (Figure 1b,c). Layer-by-layer fabrication involving additional spin-coating, UV exposure, and development steps may be used to generate multilayer microparticles (Figure S1, Supporting Information).

With the photolithography-based technique, the microparticles can be made in massive quantities from thousands to millions, and be either identical or uniquely encoded, ready for use in a variety of applications. The throughput is limited only by the pitch and size of microarray elements, as well as the size of the glass slide or the wafer, which could be scaled up easily with the assistance of industrial partners. In a single round of fabrication we demonstrated the production of up to 100 000 microparticles just on a 2-in. wafer, the throughput of which will increase to 3 million using an 11.8-in. wafer in the semiconductor industry.

The resulting particles can be lifted from the glass slide (Figure 1b,c) in two ways: using either an organic solvent, Remover PG (RPG), or an aqueous solution such as 1% BSA with Tris-EDTA (BSA/TE). RPG is a stripping solution based on *N*-methyl-2-pyrrolidone and is used lifting off photoresist films of SU-8, poly(methyl methacrylate) (PMMA), or polymethylglutarimide (PMGI) from silicon wafers and other lithography substrates. Microparticle release using this method is simple and has the advantage of further washing away unreacted monomers, which are also soluble in RPG. However, code features that are dependent on dye distribution within an encoded particle (e.g., codes generated by photobleaching) might be distorted by RPG-induced diffusion of dye within the microparticle in cases where dyes are neither covalently cross-linked nor physically trapped into the polymer matrix. To reduce the risk of losing code integrity by diffusion, we developed another approach using the aqueous BSA/TE lifting solution. For this method, formation of a thin polyvinylpyrrolidone (PVP) sacrificial layer on the glass lithography substrate prior to spin-coating with the thiol-ene polymer is required. Although this method has more steps, it is more useful for releasing encoded microparticles, which are intended for use in bioassays, as BSA/TE is biocompatible and does not diffuse into the particle.

We chose to aminate the microparticles so that functionalization using commercially available linkers, many of which are compatible with amine groups, may be performed in bioconjugation. Two approaches were evaluated to generate amine groups on the microparticle surface (**Figure 2**). Poly(allylamine hydrochloride) (PAH) with an average molecular weight of

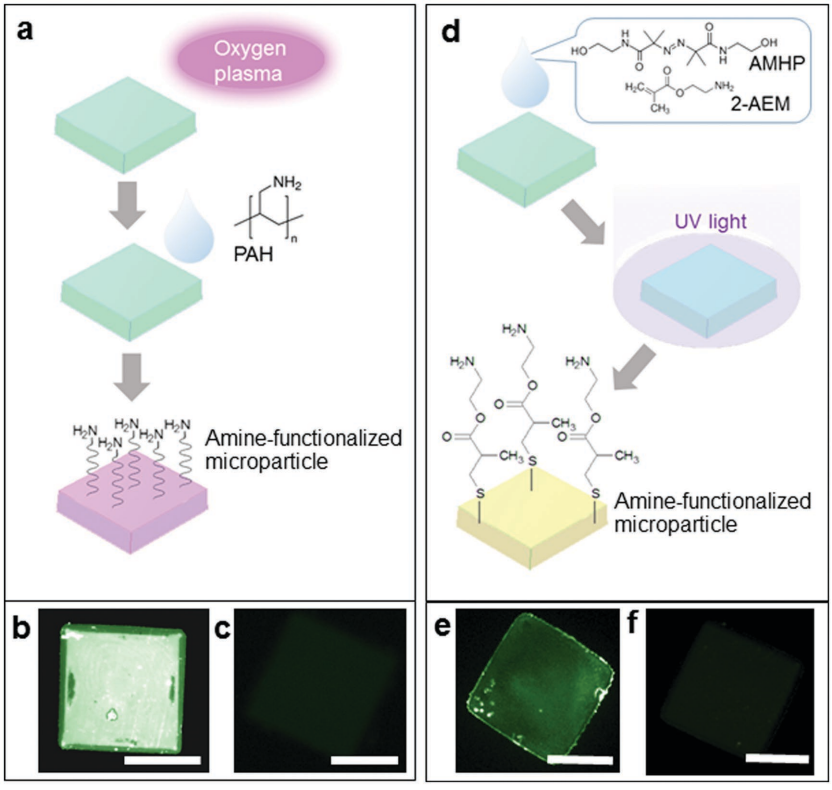

Figure 2. Functionalization of microparticles. a) Microparticles are exposed to low-pressure oxygen plasma and subsequently coated with PAH to introduce primary amine groups on the surface. Cy3-DNA is adsorbed on b) PAH-modified microparticles and on control microparticles with c) PAH coating. d) Microparticles are coated with a mixture of 2-AEM and PI and UV-induced cross-linking resulted in the amine functionalization of the microparticle surface. Cy3-DNA in green false-color adsorbed on e) 2-AEM-modified microparticles and f) on control microparticles without coating. All scale bars are 200 μm.

small 2016,
DOI: 10.1002/smll.201600456

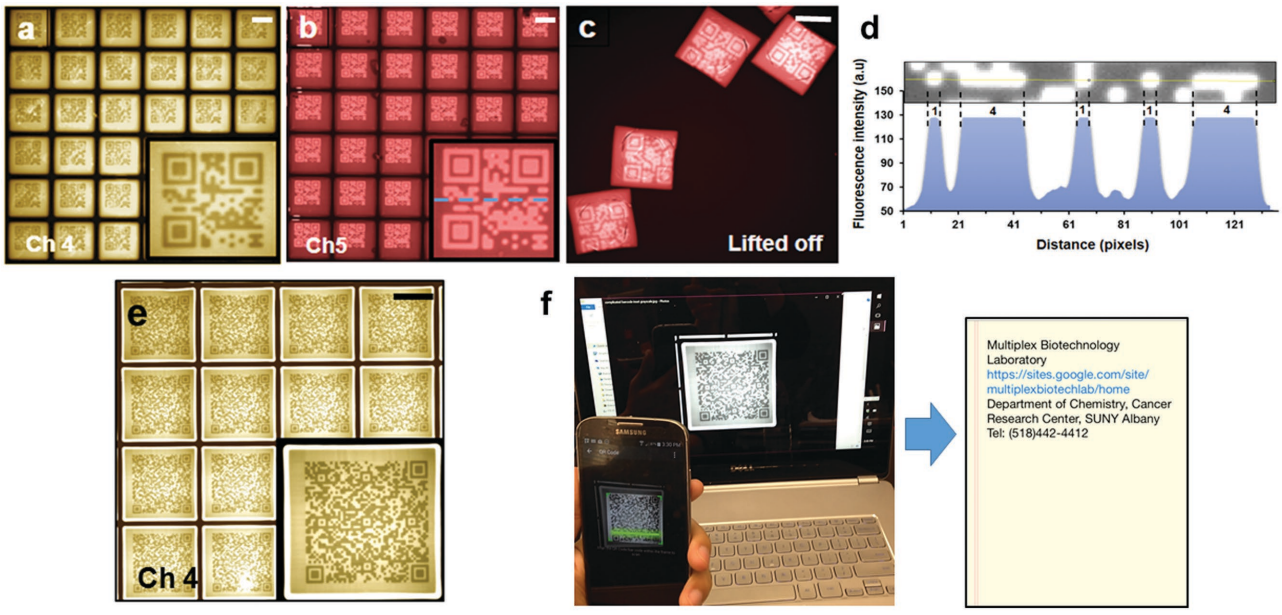

Figure 3. QR codes marked on the particles through spatially selective photobleaching. a) The 21-bit QR code is visible under a yellow/Cy3 fluorescence filter (Ch 4). b,c) The inverted QR image is visible under a red/Cy5 fluorescence filter (Ch 5), and the image is retained after lifting off. The size of QR codes is uniformly 210 μm × 210 μm with 10 μm per module. d) Profile of fluorescence intensity along a line in the photo that is cut from a QR code. The number of modules is marked between the photo and the histogram. e) 49-module QR code image taken at Cy3 excitation/emission wavelengths, with size 370 μm × 370 μm. All scale bars are 200 μm. f) The QR code is detected using a common smartphone application (left), with readout shown (right).

58 kDa was anchored to the surface after oxygen plasma treatment and 2-aminoethyl methacrylate (2-AEM) was chemically reacted with excess thiol groups through UV crosslinking. The grafting approach with PAH was not aided by UV exposure and was thus was more compatible with encoded microparticles containing fluorophores. Moreover, surface density of amine groups is ostensibly higher than that in the second method, therefore PAH grafting was chosen for DNA immobilization in our further studies.

Our coding relies on computer-assisted mask design, and various codes can be easily generated by appropriate programming. Thus, the coding capacity is mostly limited by computer power, instead of number of colors or color intensity combinations in the case of many other coding systems. With the assistance of standard lithography, it is convenient to assign a particular code to individual elements in a large array. This is demonstrated in Figure 1d that shows 4 × 4 binary holes fabricated in situ for each of the particles. The pattern array was generated by a lab-developed Matlab program. A hole indicates "1" and no hole means "0." A library of 2^{16}, or 65636, different codes can be assigned to each of the array elements simply by one coding process.

We demonstrate another encoding method via spatial selective photobleaching, which is a reproducible, rapid, and high-resolution method for encoding.[37] Photobleaching is a photochemical process in which a fluorophore molecule permanently loses the ability to fluoresce, resulting in a fading of the fluorescence intensity. We incorporated Nile Red and BDP-M fluorophores into the thiol-ene prepolymer and fabricated fluorescent microparticles pattered as ordered, segregated arrays on a glass substrate. By selectively exposing defined regions at the excitation wavelength of an incident light, the Nile Red and BDP-M particles were spatially and graphically photobleached. Nile Red has a broad fluorescence spectrum (≈520 to ≈700 nm) and the photobleached codes can be visualized under Cy3 and Cy5 filters (**Figure 3**a,b). BDP-M has a maleimide functional group that is able to react with the thiol groups on the PETMP monomer, thus, relative to Nile Red, the dye was retained in the polymer matrix more strongly after the development step in the synthesis of the fluorescent microparticles. **Figure 4**a shows the coding process in which the prepolymer was incorporated with either Nile Red or BDP-M. A photomask with a QR code array was aligned with the microparticle array and was exposed under a UV mercury lamp for 30 s in the case of Nile Red, and 10 min for BDP-M particles. The QR code on the Nile Red and BDP-M particles remained readable after 3 months of storage at room temperature and ambient levels for moisture and oxygen. We also tested the stability of BDP-M particles in aqueous medium (2% BSA in PBS) at 4 °C or in protein-free blocking buffer at room temperature and found that QR codes remained detectable after 1 week of storage (Figure S3, Supporting Information) with no significant change in apparent dye content measured by BDP-M fluorescence under a fluorescein filter. This suggests that BDP-M encoded particles to be used in bioassays may be transported or stored in these conditions, although long-term stability in aqueous solution was not monitored. The retention of BDP-M dye in the microparticles may be explained by the cross-linking of BDP-M with thiolated components of the polymer via thiol-maleimide reaction and by BDP-M's lack of ionic charge, which promotes its association with the similarly hydrophobic thiol-ene polymer matrix and limits its solubility in water.[38]

DOI: 10.1002/smll.201600456

www.MaterialsViews.com

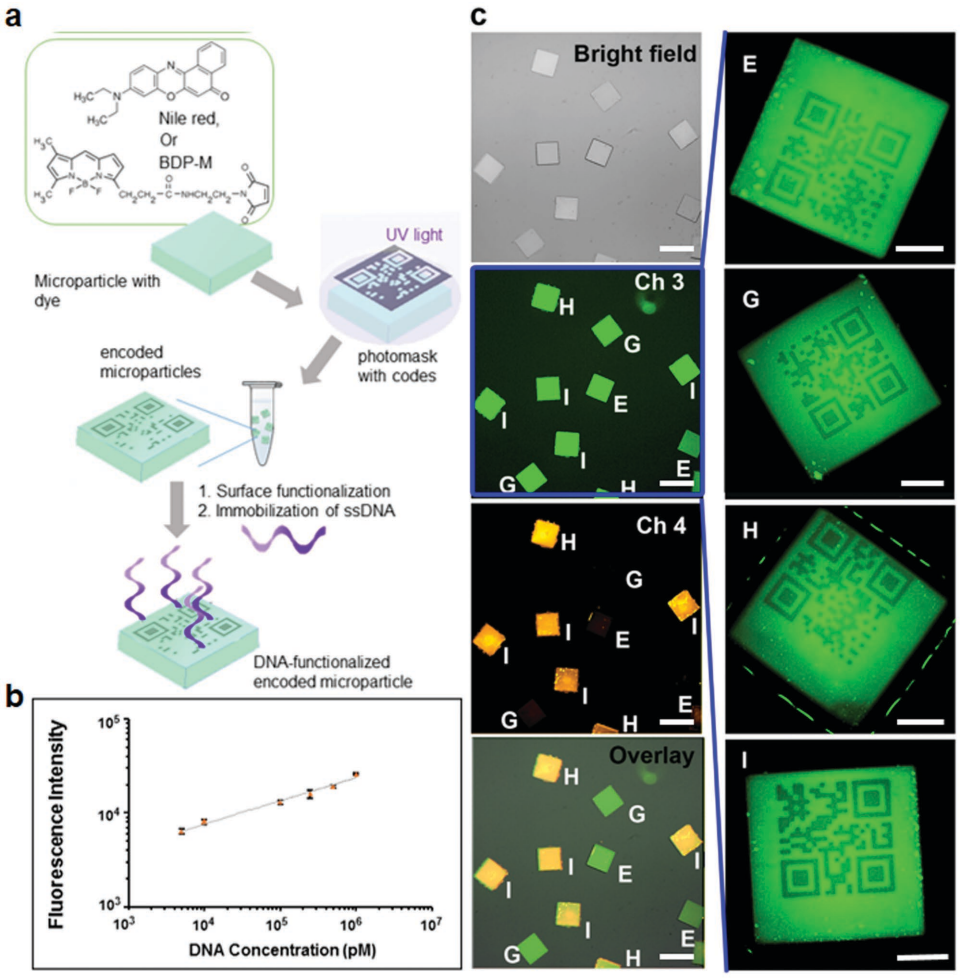

Figure 4. a) Scheme for fabricating DNA-grafted encoded microparticles. Microparticles containing Nile Red dye or BDP-M dye were exposed to UV radiation through photomasks containing multiple codes. Microparticles were released after photobleaching and subsequently functionalized with reactive groups to facilitate immobilization of single-stranded DNA on the microparticle surface. b) Logarithmic scale calibration curve for the detection of Cy3-labeled complementary DNA on DNA-grafted encoded microparticles shows a linear range of detection from 5×10^{-9} M to 1000×10^{-9} M. Error bars denote standard deviation (n = 5–8). c) Multiplexed detection of Cy3-labeled complementary DNA on DNA-tagged encoded microparticles. Images were taken under bright field, green fluorescein filter (Ch 3), and yellow/Cy3 filter (Ch 4) with green false-color for Ch3 and yellow false-color for Ch4. Scale bar = 500×10^{-6} M. An overlay of Ch3 and Ch4 images shows detected Cy3-labeled H'-DNA (100×10^{-9} M) and I'-DNA (100×10^{-9} M) in a multiplexed assay with 2 negative controls (E and G DNA). Zoomed-in images of encoded microparticles under the green filter show QR codes corresponding to E, G, H, and I DNA. Scale bars = 100 μm.

For multiplexed assays with encoded particles, we chose to use BDP-M encoded particles because the dye has a narrow fluorescence spectrum with diminished fluorescence at wavelengths >590 nm that made it suitable for fluorescence-based detection using Cy3 or Cy5 filter sets. After surface functionalization with PAH, amine-ended oligonucleotide DNAs were anchored on the BDP-M encoded microparticles via S-HyNic-S-4FB crosslinking. A specific DNA sequence was linked to each of 4 encoded microparticles (labeled as E, G, H, and I). Figure 4c shows the multiplexed detection of DNA H and I using complementary Cy3-labeled H' and I', where QR barcodes are visible under the green fluorescein filter set (channel 3), and the corresponding DNA detection occurs under the yellow/Cy3 filter set (channel 4) visualized with an inverted fluorescence microscope. We calibrated such a detection system by varying DNA concentration in DNA hybridization assay. A linear calibration curve was obtained between 5×10^{-9} M and 1000×10^{-9} M, although at low concentrations the fluorescence background of the particles under the Cy3 filter set predominates due to spectral overlap of BDP-M. We determined the limit of blank (LOB) and limit of detection (LOD) using previously described protocols[39] and obtained LOB = $0.82 \times 10^{-5} \times 10^{-9}$ M and LOD = $1.3 \times 10^{-2} \times 10^{-9}$ M. The sensitivity of the assay might be improved in the future by screening different dyes for coding or probe labeling. For instance, the end user may select a fluorescence tag for cDNA with emission wavelength >665 nm where BDP-M has no spectral overlap.

When Nile Red was incorporated in the prepolymer for coding, the patterns were inverted after development (Figure 3a–c), dramatically increasing the signal-to-noise ratio of QR barcodes. The "inversion" of the fluorescence is partially due to extraction of the hydrophobic Nile red dye from the particles by organic reagents[40] such as RPG, while

small 2016,
DOI: 10.1002/smll.201600456

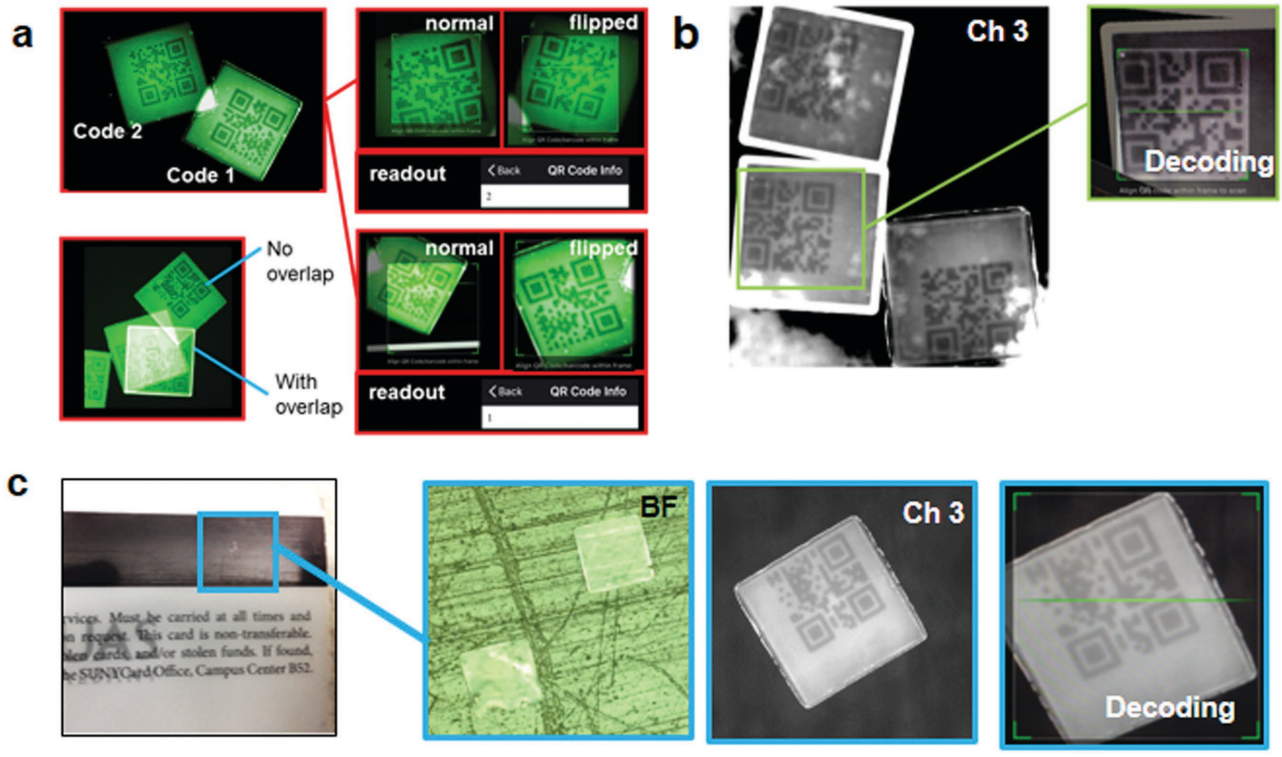

Figure 5. Rapid and controllable decoding of MiCODE particles. a) QR codes on BDP-M MiCODE particles are readable with a smartphone application regardless of whether particles are in "normal" orientation (e.g., top-side up) or "flipped" orientation (e.g., bottom-side up). Application readouts for the decoding process (less than 1 s) are shown in insets. For properly reading the codes, the particles can have certain extent of overlap as long as the QR code pattern is distinguishable. b) BDP-M MiCODE particles as potential microtaggants can be read on the surface of a bank check against a uniform low-fluorescence background under a fluorescein filter (Ch 3). c) BDP-M MiCODE particles as decodable labels on the ID shown, with zoomed-in images of particles under bright field (BF) and a green/fluorescein filter (Ch 3).

the photobleached areas possibly retained the dye molecules in highly cross-linked cavities. By this serendipitous ability of patterning, we were able to produce clear QR barcode microparticles with cellphone-readable resolution on the 330 μm particles (Figure 3). We have also manufactured a large array of QR code microparticles with a resolution of <6 μm per module (module refers to the black and white dots that make up QR barcode). The fluorescence intensity profile in Figure 3d shows that the modules can be clearly identified. Figure 3e demonstrates the high-capacity coding by 49-module QR barcodes that contain the characters of "Multiplex Biotechnology Laboratory https://sites.google.com/site/multiplexbiotechlab/home Department of Chemistry, Cancer Research Center, SUNY Albany Tel: (518)442-4412." The QR codes formed by photobleaching can be read directly by a QR barcode scanning application on a smart phone one at a time (Figure 3f). High-throughput reading of multiple QR barcodes on each image and from a batch of images is made possible with lab-developed Matlab programs using ZXing library (https://zxingnet.codeplex.com/). In **Figure 5**a, we show that the QR codes are readable on either side of the particle owing to the see-through nature of the thiol-ene polymer, the low thickness (30 μm) of the particles, and ability of the QR code to be read in different orientations, even without needing to focus the entire code area while decoding using a smartphone application. This feature is useful because flipping and overlapping of particles are inevitable in the functionalization process and bioassay applications, and the flexibility of QR decoding allows reading of every particle bearing a code as long as particles are spread out in a monolayer on a nonautofluorescent, transparent substrate, such as a clean glass slide. With the see-through particles, it is easy to distinguish between overlaps and non-overlaps, thus errors in quantifying fluorescence readouts in bioassays are avoided by setting a threshold for the BDP-M fluorescence intensity corresponding to a non-overlapping MiCODE particle. For instance, once the BDP-M-based non-overlapping codes are checked under a fluorescein filter, readout of Cy3-tagged hybridized cDNA under a Cy3 filter may be processed. We further explore the utility of the QR-encoded BDP-M particles as microtaggants by placing them on substrates that require protection against counterfeiting, such as a bank check (Figure 5b) and an identification (ID) card (Figure 5c). The QR codes are readable against a uniform, barely fluorescent background. In Figure 5b, some of the QR codes on particles are not clear because of the lack of uniformity of the black low-fluorescence ink in the background of the bank check, but this problem may be circumvented by introducing a thin layer of polymer films, inks, or dyes with low fluorescence background when immobilizing or adhering QR-encoded microtaggants on different substrates.

DNAs can be grafted on the microparticles not only by coating the whole particle surface as demonstrated above, but also by microcontact printing, which generates

DOI: 10.1002/smll.201600456

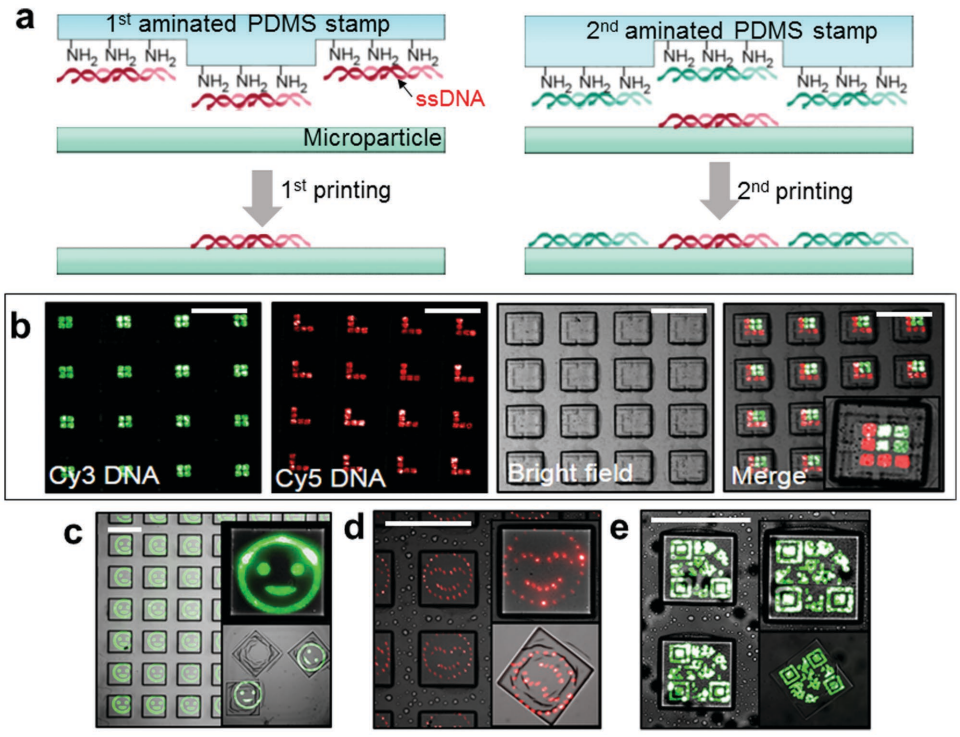

Figure 6. a) DNA printing scheme showing inking of an aminated PDMS stamp and microcontact printing of oligonucleotides on the MiCODE surface with one or multiple stampings. b) Demonstrated example of multiplex DNA microarrays on the microparticles through multi-step printing. c–e) Smiley face and QR barcode printing of Cy3-labeled ssDNA (green) and Cy5-labeled ssDNA (red) on MiCODE particles before lifting and after lifting. The smallest features for d) and e) are 15 μm. The upper panel of inset images is the zoomed-in view of a printed microparticle, and the lower panel is the zoomed-in view of a lifted microparticle in PBS. All scale bars are 500 μm.

custom-designed patterns on each of the microparticles. **Figure 6**a–d shows Cy3- and Cy5-tagged oligo DNAs sequentially printed on microparticles using polydimethylsiloxane (PDMS) stamps. A full QR code with 21 modules can also be printed on them. Printed ssDNA was stable on the microparticles both before lifting and after lifting for up to 2 weeks, after which the intensity was not monitored. It is found that the fluorescence intensity by printing is comparable to that of the coated DNA arrays in Figure 4 as well as to commercial spotted DNA arrays.

3. Conclusions

We developed a facile, versatile MiCODE technique for fabricating encoded microparticles in a high-throughput fashion, which may enhances their utility in bioassay and labeling applications. The MiCODE microparticles are fabricated by standard photolithography, leveraging the currently available semiconductor industry facilities for future scale-up manufacturing. Since the particles are not autofluorescent, fluorescence encoding strategies including spatial photobleaching for generating QR codes can be adopted. The MiCODE particle surface is chemically reactive and we have demonstrated its compatibility with biofunctionalization by grafting DNA probes on particles through chemical modification and microcontact printing with high probe density. We demonstrated the use of DNA-grafted QR encoded microparticles for a multiplexed assay detecting oligo DNAs. We have also shown tagging applications of MiCODE particles that are compatible with quick decoding using cellphone applications. Our technology is universal, simple, cost-effective, and can be fully automated for in-parallel production. We envision that suspended MiCODE microparticles can find broad applications in fields of drug screening, analysis of biomarkers for studies in genetics and signaling, and in labeling consumer goods.

4. Experimental Section

Materials: Pentaerythritol tetra (3-mercaptopropionate) (PETMP) was purchased from Tokyo Chemical Industry. Dimethyl sulfoxide (DMSO), benzophenone, and bovine serum albumin (BSA) were purchased from Fisher Scientific. 1,3,5-Triallyl-1, 3,5-triazine-2, 4,6(1H, 3H, 5H)-trione (TATATO), 2-hydroxy-2-methylpropiophenone (HMPP), TWEEN 20, poly(allylamine hydrochloride) (PAH), *N,N*-dimethylformamide (DMF), and 2-aminoethyl methacrylate hydrochloride (2-AEM) were purchased from Sigma–Aldrich. SU-8 2025, SU-8 developer (1-methoxy-2-propanol acetate), Remover PG (*N*-methyl-2-pyrrolidone solvent, RPG), and OmniCoat (cyclopentanone, propylene glycol methyl ether) were purchased from MicroChem (Westborough, MA). Phosphate buffered saline (PBS, pH 7.4), methanol, isopropyl alcohol (IPA), hydrogen peroxide, and sulfuric acid were purchased from VWR. Sylgard 184 silicone elastomer kits (PDMS) were purchased from Ellsworth Adhesives (Germantown, WI). 9-(diethylamino) 5H-benzo [α]phenoxazin-5-one (Nile Red) was purchased from Chem-Impex.

small 2016,
DOI: 10.1002/smll.201600456

BODIPY-FL-*N*-(2-aminoethyl)maleimide (BDP-M), protein-free blocking buffer, and Zeba Desalting Columns (7 kDa molecular weight cut-off) were purchased from Thermo Fisher Scientific. 2,2′-azobis(2-methyl-*N*-(2-hydroxyethyl)-propionamide (AMHP) was purchased from Wako Chemicals USA. Oligonucleotides used in this study (Table S4, Supporting Information) were purchased from Integrated DNA Technologies (Coralville, IA). The amine-reactive linkers succinimidyl-6-hydrazino-nicotinamide (S-HyNic) and N-succinimidyl-4-formylbenzamide (S-4FB) were obtained from Solulink (San Diego, CA).

Fabrication of Microparticle Arrays: MiCODE microparticles were fabricated using lithographic methods with a photoresist-like polymer comprised of PETMP and TATATO, with HMPP as the photoinitiator. The fabrication of large microparticles above 100 µm was based on a prepolymer mixture of PETMP and TATATO with a thiol-allyl functional group ratio of 1.6:1. For small features less than 100 µm, a thiol-allyl ratio at 0.77:1 was employed for higher spatial resolution. For encoded microparticles, the prepolymer formulation had a ratio 1.6:1 with either 0.12% (wt/wt) Nile Red or 2.5×10^{-4}% (wt/wt) BDP-M. All the prepolymers contained 1% (wt/wt) HMPP.

Silicon wafers and glass slides were cleaned using piranha solution (3:1 mixture of 96% H_2SO_4 and 30% H_2O_2) at 90 °C for 20 min, rinsed with copious amounts of DI water and IPA, and dried under a stream of nitrogen. The prepolymer was poured on either a wafer or a glass slide, and was immediately spun at 500–700 rpm for 30 s with a spin coater (WS-650MZ-23NPPB, Laurell). For encoded microparticles, the prepolymer was poured on a PVP sacrificial layer. To generate the PVP layer, a clean glass slide was spin-coated with a solution of 5% (wt/wt) PVP in DMF at 3000 rpm for 30 s, and later heated to 170 °C to remove the DMF solvent. For small microparticles (15 µm), the prepolymer mixture was placed on a glass slide with a layer of OmniCoat generated following the manufacturer's instructions.

A photomask was placed on the spun prepolymer with a space of 130 µm in between. The collimated UV light generated by a UV lamp (OmniCure Series 1000, Lumen Dynamics) penetrated only through the transparent patterns on the photomask and initiated the crosslinking of thiol and allyl groups. Specific spin speed and UV intensity for the fabrication of different sizes are shown in Table S1 (Supporting Information). SU-8 developer was then utilized to wash off the unreacted monomers; the glass slide or wafer with the cured polymer was dipped into a glass container with ≈20 mL of developer, placed on a shaker for 1–2 min, and blown dry.

Microparticles without fluorophores were further subjected to post-exposure under UV light (power 50%, 5 min) in order to maximize the crosslinking of unreacted groups remaining in the structure. This step increased the mechanical strength of the particles.

For the fabrication of a second layer onto the micropallets, we tested various thiol-allyl prepolymer compositions and decided to use a ratio of 2.25:1 because other compositions often resulted in defective structures. The spin rate was raised to 1500 rpm to achieve a thin wall ≈20 µm thick on 330 µm microparticles. A custom setup was employed for mask alignment to achieve precise overlay of the features on the photomask to the first-layer features on a glass slide or wafer. After UV exposure for 35 s at power 30%, the second layer's features were developed in SU-8 developer for ≈1 min and blown dry with nitrogen.

Microparticle Release: Various methods for releasing microparticles were used. Larger microparticles (>15 µm) fabricated on slides without a sacrificial layer were released by immersing the slide in RPG with strong agitation for 10 min. The 15 µm microparticles required a more rigorous method that involved incubating the slide in RPG at 80 °C for 30 min with agitation. The microparticle suspension in RPG was centrifuged at 3000 rpm for 4 min, and washed with 0.1% TWEEN in PBS (pH 7.4). The washing procedure was repeated to remove residual RPG. Microparticles that had a propensity for aggregation were alternatively resuspended in 1% BSA in Tris-EDTA buffer with 0.1% TWEEN 20 (BSA/TE, pH 7.4). Microparticles fabricated on a PVP sacrificial layer were lifted off simply by immersing the slides in 1%BSA/TE (pH 7.4).

Photobleaching: Microparticles containing Nile Red or BDP-M were fabricated as described above. After development, the microparticle arrays were exposed through another photomask to collimated UV light. The Nile Red fluorophore has a faster rate of photobleaching compared to BDP-M; microparticles with Nile Red were exposed to 100 mW UV with power 100% for 30 s, while BDP-M microparticles required power 100% for 10 min. The UV exposure transferred the micropatterns onto the particles in the form of darkened areas that corresponded to photobleached fluorophores. The microparticles were subsequently released and resuspended in 1% BSA/TE (pH 7.4) or PBS.

Design of QR-Pattered Photomask: The photomask was designed using AutoCAD software. The QR Codes were generated using a free online-based QR Code Generator from the Zebra Crossing (ZXing) Project (http://zxing.appspot.com/generator). With this generator, the QR size, type of character encoding, and error correction level (L, M, Q, H) were selected. The design of the QR Code was saved in the Portable Network Graphics (PNG) format, then converted into Drawing (DWG) format that can be opened in AutoCAD. The code array in DWG was subsequently compiled into a single mask. This arrangement was superimposable on the photomask design used for fabricating microparticles that were also segregated into arrays.

Amination of Microparticle Surface: Released microparticles from arrays (330 µm flat squares) were spread out on an oxygen plasma-treated polydimethylsiloxane (PDMS) slab, washed with water, and air-dried. The oxygen plasma (PDC-32G, Harrick Plasma) rendered the PDMS hydrophilic, so that aqueous grafting solutions were able to permeate the pores of the PDMS on the underside of flat microparticles, thereby permitting functional group incorporation on both the top and bottom faces of the particles.

To functionalize microparticles with PAH, particles were exposed to low-pressure oxygen plasma for 5 min and the slab was immersed in 300 mg mL^{-1} PAH in PBS for 20 min. The PAH grafting solution was washed off using water and the particles were resuspended in 1% BSA/TE (pH 7.4). In another method, the particles' surface thiol groups were conjugated to 2-AEM. A grafting solution with 17 mg mL^{-1} 2-AEM and 2.2 mg mL^{-1} AMHP in PBS, pH 7.4 was poured on the particles. The particles were exposed to UV with power 100% for 5 min, washed with water, and air-dried. UV exposure allowed for the AMHP-mediated reaction of the particles' excess thiol groups with the methacrylate group on 2-AEM.

To demonstrate the incorporation of primary amine groups by either method on the particle surface, microparticles were incubated with 1×10^{-6} M 5′-Cy3 modified DNA in 1% BSA/TE for an hour, and an increase in yellow fluorescence was observed under

DOI: 10.1002/smll.201600456

a fluorescence microscope after polyanionic DNA adsorbed to the positively charged aminated surface.

DNA Microcontact Printing: SU-8 masters for casting of the PDMS stamps were fabricated on 2-in. diameter silicon wafers. SU-8 2025 was spun on the wafer at 300 rpm for 10 s ramping to 1300 rpm for 30 s. The wafer was then pre-baked for 9 min at 95 °C, followed by exposure to collimated UV light through a patterned photomask for 30 s at power 5. The wafer was post-baked for 9 min at 95 °C and allowed to cool slowly for 20 min. Next, the wafer was developed in SU-8 developer for 5 min, rinsed with IPA, and blown dry with a stream of nitrogen. The mold was hard baked for 10 min at 160 °C and cooled slowly.

PDMS stamps were prepared by casting Sylgard 184 prepolymer on an SU-8 mold with the desired stamp features. The PDMS was allowed to cure for 90 min at 80 °C in an oven, and then the PDMS stamps were peeled off from the master. Next, the surface of the PDMS stamps was oxidized using oxygen plasma for 10 min. After this step, the PDMS stamps were immersed in methanol containing 100×10^{-3} M benzophenone and 100×10^{-3} M 2-AEM for 30 min at room temperature in a humidified chamber. The stamps were then inked with 5×10^{-6} M of the desired ssDNA dissolved in 50% DMSO in DI water for 45 min at room temperature in a humidified chamber. Finally, the stamps were blown dry and used immediately. Before stamping, the fabricated array was treated with oxygen plasma (PDC-32G, Harrick Plasma) for 5 min to generate reactive groups on the surface. The inked DNA stamps were then brought into conformal contact for 30 s with the microparticle surface using a custom-built alignment microscope and stage.

Grafting of DNA Probes on Encoded Microparticles: Microparticles bearing QR codes in BDP-M were functionalized with PAH as described above. The amine-functionalized particles were resuspended in PBS (pH 7.4). The amine surface was modified with hydrazine functional groups by reacting ≈1000 particles with 2×10^{-3} M S-HyNic (from a stock solution in DMF) in PBS with 2.5% (v/v) DMF for 3 h at room temperature.

Amine-modified (5′-Amine) oligonucleotides with sequences E, G, H, and I were reacted with S-4FB in a 1:400 (DNA:S-4FB) mole ratio in PBS with 15% (v/v) DMF for 3 h at room temperature. The primary amine groups on the oligonucleotides reacted with S-4FB, incorporating a 4-formylbenzamide linker on each oligonucleotide strand. Excess S-HyNic was removed by washing the particles in citrate buffer (50×10^{-3} M trisodium citrate, 150×10^{-3} M NaCl, pH 6.0). Unreacted S-4FB was separated from the S-4FB-DNA by performing a buffer exchange with citrate buffer using Zeba Desalting Columns according to manufacturer's instructions. S-4FB-modified oligonucleotides were then combined with S-HyNic-modified encoded microparticles with a final concentration of 0.067×10^{-3} M S-4FB-DNA in citrate buffer. The S-4FB-S-HyNic coupling reaction took 12 h at room temperature. The resulting DNA-grafted microparticles were later used in a multiplexed bioassay.

Multiplexed DNA Hybridization Assay with Encoded Microparticles: A calibration curve was constructed by hybridizing 5×10^{-9} M–1000×10^{-9} M Cy3-labeled complementary DNA with sequences E', G', H', and I' in 1% BSA/TE on DNA-functionalized BDP-M encoded particles. Four batches of DNA-functionalized encoded microparticles were prepared with E, G, H, and I DNA immobilized on the particle surface. Each batch of DNA-functionalized microparticles had a unique QR code that was visible when the particles were illuminated under a fluorescein fluorescence filter. Cy3-labeled DNA H' and I' (100×10^{-9} M in 1% BSA/TE at pH 7.4) were combined a mixture of encoded microparticles bearing E, G, H, and I DNA. After 1.5 h, the hybridization of Cy3-labeled DNA on microparticles was observed under a yellow/Cy3 fluorescence filter.

Microscopy Imaging and Analysis: Encoded microparticles with Nile-Red or BDP-M fluorophores as well as microparticles with printed fluorescent ssDNA were observed with an inverted fluorescence microscope (IX73, Olympus). The microscope was equipped with three fluorescence filter sets: a green fluorescein filter set (U-FF, Olympus; excitation filter 450–490 nm, dichroic 500 nm long pass, emission 520 nm long pass), a yellow/Cy3 filter set (U-FF, Olympus; excitation filter 528–553 nm dichroic 565 nm long pass, emission 590–650 nm), and a red Cy5 filter set (U-FF, Olympus; excitation filter 590–650 nm, dichroic 660 nm long pass, emission 665–740 nm). A microscope objective (UPlanSApo, Olympus, 4×/0.16; UPlanFLN, Olympus, 10×/0.30/Ph1; UCPlanFLN, Olympus, 20×/0.70/Ph2) was used to collect fluorescence light. A digital camera (Zyla sCMOS, Andor) mounted on the microscope was used to capture images using Andor SOLIS software.

Images of fluorescent microparticles containing BDP-M were acquired using the fluorescein filter set and rendered in green pseudo-color. Nile red microparticle images taken using the Cy3 filter set were rendered in yellow pseudo-color, while those using the Cy5 filter set were shown with red pseudo-color. All color channel manipulations were done using Adobe Photoshop. The fluorescence profile of images was processed using ImageJ (National Institute of Health). For the multiplexed hybridization assay, images were acquired using the same acquisition settings with a 16-bit (0-65,535 scale) output. Median fluorescence intensity of microparticles under the yellow/Cy3 filter was taken as a measure of the concentration of detected DNA. The same parameters were used for analysis of all particles.

Determination of Limit of Blank and Limit of Detection: The LOB and LOD were calculated using a previously reported method.[39] The LOB (Equation (1)) was calculated from the mean ($\text{mean}_{\text{blank}}$) and standard deviation (SD_{blank}) of the fluorescence signals of blank microparticles:

$$\text{LOB} = \text{mean}_{\text{blank}} + 1.645(\text{SD}_{\text{blank}}) \quad (1)$$

The LOB corresponds to the highest apparent DNA concentration expected to be detected based upon fluorescence measurements of replicates of the blank, which were DNA-functionalized microparticles incubated with 0×10^{-9} M Cy3-tagged cDNA.

The LOD (Equation (2)) was calculated by incrementing the LOB with the standard deviation of fluorescence signals (SD_{lc}) obtained from microparticles that assayed low concentrations (1×10^{-9} M–5×10^{-9} M) of DNA:

$$\text{LOD} = \text{LOB} + 1.645(\text{SD}_{\text{lc}}) \quad (2)$$

Supporting Information

Supporting Information is available from the Wiley Online Library or from the author.

DOI: 10.1002/smll.201600456

Acknowledgements

L.M.S.R. and M.H. contributed equally to this work. The authors declare no competing financial interest. The authors thank Dr. David Spiegel from Yale University for helpful discussion and constructive advice. This work was supported by the Presidential Initiatives Fund for Research and Scholarship and startup fund from SUNY Albany to J.W.

[1] J. D. Hoheisel, *Nat. Rev. Genet.* **2006**, *7*, 200.
[2] L. Wang, P. C. H. Li, *Anal. Chim. Acta* **2011**, *687*, 12.
[3] Y. Zhang, L. B. Qiao, Y. K. Ren, X. W. Wang, M. Gao, Y. F. Tang, J. J. Xi, T. M. Fu, X. Y. Jiang, *Biomicrofluidics* **2013**, *7*, 034110.
[4] H. Lee, J. Kim, H. Kim, J. Kim, S. Kwon, *Nat. Mater.* **2010**, *9*, 745.
[5] G. C. Le Goff, R. L. Srinivas, W. A. Hill, P. S. Doyle, *Eur. Polym. J.* **2015**, *72*, 386.
[6] S. E. Chung, J. Kim, D. Y. Oh, Y. Song, S. H. Lee, S. Min, S. Kwon, *Nat. Commun.* **2014**, *5*, 3468.
[7] J. P. Nolan, L. A. Sklar, *Trends Biotechnol.* **2002**, *20*, 9.
[8] J. Lei, J. Hsu, P. Jen, D. Huang, A. Chung, L. Kao, M. Chang, C. C. Yuan, W. H. Lee, C. T. Yeh, D. Tsao, *Cancer Res.* **2014**, *74*, 4663.
[9] J. M. Schwenk, U. Igel, B. S. Kato, G. Nicholson, F. Karpe, M. Uhlen, P. Nilsson, *Proteomics* **2010**, *10*, 532.
[10] P. W. Stevens, C. H. J. Wang, D. M. Kelso, *Anal. Chem.* **2003**, *75*, 1141.
[11] B. He, S. J. Son, S. B. Lee, *Anal. Chem.* **2007**, *79*, 5257.
[12] Y. Zhao, Y. Cheng, L. Shang, J. Wang, Z. Xie, Z. Gu, *Small* **2015**, *11*, 151.
[13] H. Lee, J. Kim, H. Kim, J. Kim, S. Kwon, *Nat. Mater.* **2010**, *9*, 745.
[14] S. C. Chapin, P. S. Doyle, *Anal. Chem.* **2011**, *83*, 7179.
[15] D. C. Appleyard, S. C. Chapin, P. S. Doyle, *Anal. Chem.* **2011**, *83*, 193.
[16] N. W. Choi, J. Kim, S. C. Chapin, T. Duong, E. Donohue, P. Pandey, W. Broom, W. A. Hill, P. S. Doyle, *Anal. Chem.* **2012**, *84*, 9370.
[17] K. W. Bong, S. C. Chapin, P. S. Doyle, *Langmuir* **2010**, *26*, 8008.
[18] J.-T. Wang, J. Wang, J.-J. Han, *Small* **2011**, *7*, 1728.
[19] S.-H. Song, K. Kim, S.-E. Choi, S. Han, H.-S. Lee, S. Kwon, W. Park, *Opt. Lett.* **2014**, *39*, 5162.
[20] K. S. Paulsen, D. Di Carlo, A. J. Chung, *Nat. Commun.* **2015**, *6*, 6976.
[21] L. N. Kim, M. Kim, K. Jung, H. J. Bae, J. Jang, Y. Jung, J. Kim, S. Kwon, *Chem. Commun.* **2015**, *5*, 12130.
[22] S. Han, H. J. Bae, J. Kim, S. Shin, S.-E. Choi, S. H. Lee, S. Kwon, W. Park, *Adv. Mater.* **2012**, *24*, 5924.
[23] S. E. Chung, W. Park, H. Park, K. Yu, N. Park, S. Kwon, *Appl. Phys. Lett.* **2007**, *91*, 041106.
[24] S. Park, H. J. Lee, W. G. Koh, *Sensors* **2012**, *12*, 8426.
[25] S. W. Han, E. Jang, W. G. Koh, *Sens. Actuators, B* **2015**, *209*, 242.
[26] D. Dendukuri, D. C. Pregibon, J. Collins, T. A. Hatton, P. S. Doyle, *Nat. Mater.* **2006**, *5*, 365.
[27] Y. Jung, H. Lee, T.-J. Park, S. Kim, S. Kwon, *Sci. Rep.* **2015**, *5*, 15629.
[28] J. V. Crivello, E. Reichmanis, *Chem. Mater.* **2014**, *26*, 533.
[29] M. H. Stenzel, *ACS Macro Lett.* **2013**, *2*, 14.
[30] Q. Li, H. Zhou, C. E. Hoyle, *Polymer* **2009**, *50*, 2237.
[31] C. F. Carlborg, A. Vastesson, Y. T. Liu, W. van der Wijngaart, M. Johansson, T. Haraldsson, *J. Polym. Sci., Polym. Chem.* **2014**, *52*, 2604.
[32] E. C. Hagberg, M. Malkoch, Y. B. Ling, C. J. Hawker, K. R. Carter, *Nano. Lett.* **2007**, *7*, 233.
[33] V. S. Khire, Y. Yi, N. A. Clark, C. N. Bowman, *Adv. Mater.* **2008**, *20*, 3308.
[34] C. E. Hoyle, T. Y. Lee, T. Roper, *J. Polym. Sci. A* **2004**, *42*, 5301.
[35] C. F. Carlborg, T. Haraldsson, K. Oberg, M. Malkoch, W. van der Wijngaart, *Lab Chip* **2011**, *11*, 3136.
[36] J. Yoon, K. J. Lee, J. Lahann, *J. Mater. Chem.* **2011**, *21*, 8502.
[37] K. Braeckmans, S. C. De Smedt, C. Roelant, M. Leblans, R. Pauwels, J. Demeester, *Nat. Mater.* **2003**, *2*, 169.
[38] N. Dorh, S. Zhu, K. B. Dhungana, R. Pati, F.-T. Luo, H. Liu, A. Tiwari, *Sci. Rep.* **2015**, *5*, 18337.
[39] D. A. Armbruster, T. Pry, *Clin. Biochem. Rev.* **2008**, *29*, 49.
[40] P. Greenspan, S. D. Fowler, *J. Lipid Res.* **1985**, *26*, 781.

Received: February 11, 2016
Revised: April 4, 2016
Published online: